Sustainable Structures
ISSN: 2789-3111 (Print); ISSN: 2789-312X (Online)
http://www.sustain-dpl.com/journal/sust
DOI: 10.54113/j.sust.2025.000080

ORIGINAL ARTICLE

Effect of rice husk ash on compressive strength of sustainable pervious concrete and prediction model using machine learning algorithms

Navaratnarajah Sathiparan[a,*], Pratheeba Jeyananthan[b], Daniel Niruban Subramaniam[a]

[a] Department of Civil Engineering, Faculty of Engineering, University of Jaffna, Jaffna 40000, SriLanka
[b] Department of Computer Engineering, Faculty of Engineering, University of Jaffna, Jaffna 40000, SriLanka
[*]Corresponding Author: Navaratnarajah Sathiparan. Email: sakthi@eng.jfn.ac.lk

Abstract: This study investigates the effect of rice husk ash (RHA) on compressive strength of pervious concrete and explores the use of machine learning (ML) for forecasting its strength. An inclusive dataset encompassing various parameters of pervious concrete with RHA was compiled from published research. This data was utilized to develop and assess ML models for predicting compressive strength. Six different algorithms, including Artificial Neural Network (ANN), Boosted tree regression (BT), K-nearest neighbors (KNN), Linear regression (LR), Support Vector Regression (SVR), and Extreme Gradient Boosting (XGB), were investigated. The findings indicate an optimal RHA content for achieving maximum strength, with compressive strength generally increasing to a 10% replacement level and then decreasing with further RHA substitution. The analysis showed that the SVR model was the most effective and reliable option for prediction. SVR model achieved greater performance related to other models, exhibiting a higher coefficient of determination and lower values for Root Mean Square Error and Mean Absolute Error. The study shows that SVR model can accurately identify how different factors in data influence each other. This makes it a valuable tool for predicting how strong pervious concrete is with RHA under compression. SHAP (SHapley Additive exPlanations) analysis showed that aggregate size significantly affects compressive strength, followed by water-to-binder ratio and curing period.

Keywords: Pervious concrete, rice husk ash, machine learning, compressive strength

1 Introduction

Pervious concrete is a unique concrete formulation engineered to facilitate rapid water drainage. Pervious concrete differs from regular concrete in that it contains numerous voids between the aggregates, allowing it to absorb water, whereas regular concrete is solid and impermeable [1]. This space, called porosity, can be between 15% and 35% of the total volume of pervious concrete [2]. Rainwater and other liquids can be transmitted through pervious concrete, reducing stormwater runoff and helping replenish groundwater supplies. This is especially useful in urban areas where many paved surfaces prevent water from naturally infiltrating into the ground [3]. Due to its ability to manage water effectively, pervious concrete is commonly used in various applications, such as driveways, parking lots, sidewalks, and recreational areas. It is particularly beneficial in stormwater management systems, where it helps mitigate the effects of heavy rainfall and urban heat islands. Additionally, pervious

Received: 15 November 2024; Received in revised form: 15 February 2025; Accepted: 8 August 2025

concrete can be employed in green infrastructure projects, contributing to sustainable urban design initiatives that aim to integrate natural processes into the built environment.

Recent studies have explored mechanical performance of various concrete formulations, highlighting the significance of incorporating alternative materials to enhance structural integrity. Zhang et al. [4] investigated the performance of basalt fiber-reinforced recycled aggregate concrete subjected to high temperatures, highlighting the potential of these materials to enhance durability. Similarly, another investigation by Zhang et al. [5] examined the eccentric compression performance of basalt fiber-reinforced recycled aggregate in tubular columns, further emphasizing the versatility of composite materials in construction applications.

Pervious concrete inherently uses more cement than traditional concrete due to the absence of fine particles that fill gaps. Supplementary cementitious materials (SCMs) partly substitute Portland cement, lowering the overall clinker factor (a measure of environmental impact in cement production) [6]. Manufacturing of Portland cement is a significant source of CO_2 emissions. Using less cement and incorporating SCMs, pervious concrete can have a smaller carbon footprint [7]. SCMs like fly ash or silica fume can react with hydration products of cement, leading to denser and stronger concrete. This is crucial for pervious concrete as it needs adequate strength despite high void content [8]. Some SCMs can improve workability of pervious concrete mix, facilitating placement and finishing during construction. Certain SCMs like metakaolin can improve resistance of pervious concrete to chemicals like acids, enhancing its long-term performance [9]. SCMs can often be cheaper than Portland cement, lowering overall material cost of pervious concrete [10].

Specific benefits of SCMs in pervious concrete be contingent on the chosen material and its properties. Beyond the influence of SCMs, several other aspects affect pervious concrete's properties [11]. Mix design plays a critical role, with a lower water-to-cement ratio leading to a stronger and less permeable concrete, but also one that's trickier to work with [12]. Nominal and distribution of size of coarse aggregates are also critical, as a well-graded mix with minimal fine particles optimizes drainage while maintaining strength [13]. Curing with proper moisture management is essential for pervious concrete to reach its full potential and prevent cracking. Additionally, admixtures can be used for specific purposes, and compaction methods must be tailored to avoid reducing this unique concrete type's crucial porosity and drainage capacity [13]. Engineers can achieve optimal pervious concrete for various applications by carefully considering all these factors.

Regular concrete is well-understood, but pervious concrete's high porosity and reliance on a specific mix design make it more complex. Traditional methods for predicting strength may only partially capture these nuances [14]. Machine learning (ML) analyses large datasets of past pervious concrete mixes and their corresponding compressive strengths. This allows it to identify hidden patterns and relationships between various mix design factors and resulting strength [15]. ML models can learn from large amounts of data, potentially leading to more precise compressive strength forecasts than traditional methods based on limited formulas or rules of thumb. As research explores new SCMs or other concrete components, ML models can readily adapt to incorporate this new data and improve their predictive capabilities [16]. ML can analyse various mix design options and predict their strengths, allowing engineers to optimize concrete mixes for specific strength requirements while potentially reducing material costs.

Recent advancements in civil engineering have witnessed a growing interest in leveraging ML techniques for estimating performance characteristics of building materials [17-20]. This trend is particularly relevant for complex material behaviours, such as the association between RHA replacement and strength. **Table 1** summarizes existing study on forecasting models for compressive strength of SCMs blended pervious concrete, highlighting the application of various ML techniques. Sudhir et al. [21] and Ahmad et al. [22] achieved high accuracy (R^2 approaching 0.99) using ANN for compressive strength prediction. However, these investigations were limited by datasets derived from a single experimental program. Sathiparan et al. [16, 23] predicted the compressive strength of SCMs such as fly ash, metakaolin, and silica fume blended pervious concrete using ML algorithms. Their studies collected data from various published literature showing that Extreme Gradient Boosting (XGB) performed better than other models. This study recognizes a gap in the current literature regarding

developing a specifically tailored ML model for forecasting compressive strength of pervious concrete with rice husk ash (RHA).

Table 1. Overview of the ML models utilized for predicting the compressive strength of SCMs blended pervious concrete

SCMs used	Ref	Data points	MLs used
Fly ash	Sathiparan et al. [23]	437	LR, ANN, BT, SVR, RF & XGB
Fly ash, Silica fume	Yu et al. [24]	123	CNN & BPNN
Ground Granulated Blast-furnace Slag	Sudhir Kumar et al. [21]	18	ANN
Metakaolin	Sathiparan et al. [16]	131	ANN, BT, RF & XGB
Silica fume	Sathiparan et al. [25]	222	LR, ANN, BT, KNN, SVR, RF & XGB
Silica fume	Le et al. [26]	164	XGB, RF, SVR, ANN
Waste glass powder	Ahmad et al. [22]	99	LR, NLR, ANN

RHA is a byproduct of agricultural activities, and utilizing it lessens the need for cement production with a high environmental footprint. RHA offers potential advantages over other SCMs like fly ash, metakaolin, and silica fumes when used as a cement replacement. Rice husk is a waste product from rice production, creating a plentiful and sustainable source of RHA compared to byproducts from industrial processes like fly ash [27]. Also, RHA can improve early-age strength of concrete compared to some SCMs, like FA, which can see slower strength development initially. This can be beneficial for projects requiring faster turnaround times. Research indicates that RHA can enhance the workability of fresh mixes, facilitating easier placement and handling during construction [28]. Studies have shown that up to a certain percentage (typically around 10-12%) of cement replacement with RHA can improve compressive strength [29, 30]. In addition, RHA is generally cheaper than cement and other SCMs that can reduce cost of pervious concrete production [29]. As mentioned earlier, the strength of pervious concrete depends on various factors; a proper mix design is essential to optimize concrete mixes for specific strength requirements.

Several studies focused on predicting compressive strength of RHA blended concrete. Kashan et al. [31] reported that hybrid machine-learning algorithms can accurately predict compressive strength of RHA blended concrete. These models significantly outperform traditional methods. Key factors influencing strength include cement, curing age, water, and RHA content. The optimal RHA content for maximum strength is between 25-175 kg/m ^{3}. This research provides valuable insights for optimizing RHA blended concrete mix designs and improving construction efficiency and safety. Despite increasing use of RHA as a SCM in various concrete formulations, there is notable deficiency of research specifically focusing on forecast of compressive strength of RHA-blended pervious concrete. Predicting strength using ML algorithms is crucial for several reasons. First, accurate predictions can lead to optimized mixed proportion that enhance performance and sustainability, reducing material costs and environmental effect. Second, ML techniques can identify complex associations among various mix parameters and compressive strength that traditional methods may overlook. This predictive capability is mainly vital in the context of sustainable construction practices, where efficiency and resource conservation are paramount. In this study, the capability of ML is explored to forecast compressive strength of previous concrete, which incorporates RHA as an additional ingredient. The data is collected from pervious concrete mixes from various published research sources. Performance of six different ML techniques is compared to find the most accurate prediction method. Ultimately, models developed in this study offer a new method to improve accuracy of predicting strength of pervious concrete containing RHA. This could benefit engineers and construction professionals working with this type of material.

2. Methodology

2.1 Data collection

An inclusive literature exploration used reputable databases like Web of Science, Scopus, and Google Scholar. The exploration string encompassed terms related to pervious concrete ("pervious concrete", "porous concrete", "permeable concrete") and RHA ("rice husk ash", "RHA"). This strategy aimed to identify relevant studies within the title, abstract, and keywords. Following initial search, the retrieved literature underwent a thorough screening process to disregard duplicate data. This ensured that the data used for further analysis was original and non-redundant. Relevant information for constructing ML models was subsequently extracted and summarized in **Table 2**. In selecting input variables for ML models, study focused on parameters that have been widely recognized in existing literature as significant predictors for compressive strength. The chosen parameters include:

- Aggregate-to-binder ratio (Agg/B): This ratio is crucial as it influences the density and strength of the concrete mix.
- Rice husk ash-to-binder ratio (RHA/B): RHA is included because of its pozzolanic properties, which enhance strength when used within certain limits.
- Water-to-binder ratio (W/B): This ratio is vital for determining the workability and strength of the concrete, as it directly affects hydration.
- Mean aggregate size: The size of aggregates impacts the concrete's porosity and interlocking characteristics, influencing overall strength.
- Curing period: Curing conditions are essential for the development of compressive strength, as they affect the hydration process.

These variables were selected based on a review of previous studies that have demonstrated their relevance in predicting compressive strength in concrete. This comprehensive approach ensures that the model captures multifaceted interactions between different components of concrete mix. The compiled dataset encompassed 193 observations, offering a robust foundation for analysis. This comprehensive dataset encompassing various features of pervious concrete with RHA is expected to be valuable for future research and industrial applications.

Table 2. Overview of the data composed form published literature

Ref	Agg/B	RHA/B	W/B	Mean Agg. Size	Curing period	CS	No. of data
Adamu et al. [32]	5.5	0-0.1	0.40	12	3, 7, 28	4.7-7.3	6
Balasubramani et al. [33]	6, 8, 10	0.03-0.09	0.45	15	7, 28	2.2-9.4	18
Hesami et al. [34]	4.4	0-0.12	0.27	10.7	28	13.6-17.7	4
Kim et al. [35]	6.5	0-0.35	0.20	7.5	7, 28	2.0-7.8	16
Ramadhasyah [36]	2.5	0-0.4	0.34	8.4	7, 14,28, 56, 90	14.7-35.1	25
Sai Kumar [37]	2.4	0-0.3	0.40	16	7, 28	7.5-10.9	8
Shafabakhsh and Ahmadi [38]	4.4	0-0.12	0.34	7.5	28	14.5-20.6	7
Shekhar and Shukla [39]	3.0	0-0.2	0.40	8	7, 14, 28	18.2-38.4	18
Shwetha [40]	5.6	0-0.3	0.42	12.5	7, 14, 28, 56	5.7-12.2	16
Subramaniam and Sathiparan [6]	2.5	0-0.2	0.30-0.45	7.5	7, 28	4.4-34.4	40
Talsania et al. [41]	4	0-0.2	0.30-0.40	15	7, 14, 28	6.4-11.0	27
Vanathi et al. [42]	6	0-0.3	0.36	14.75	7, 28	4.3-13.9	8
Overall	2.5-10	0-0.4	0.2-0.45	7.5-16	3-90	2.0-38.4	193

Experimental studies from which the data was sourced primarily involved mixing RHA with pervious concrete in varying proportions. Sample preparation involved thoroughly mixing dry ingredients, including cement, aggregates, and RHA, followed by careful addition of water. Most studies utilized a 150 mm cube for testing, while a couple of studies employed a 100 mm cube and a 150 x 300 mm cylindrical specimen. Compressive strength tests were conducted in according to established protocols, including ASTM C39 [43], BS-EN-12390 [44], and IS: 516 [45]. Samples were subjected to a uniaxial compressive load until failure, with the maximum load recorded to calculate

compressive strength. For ML model analysis, we used raw data extracted from reviewed studies. Utilizing raw data is justified as it provides a comprehensive and unaltered representation of experimental outcomes, ensuring that our model captured inherent variability and characteristics in data. This method lets for a more accurate analysis and better generalization of results.

2.2 Machine learning models

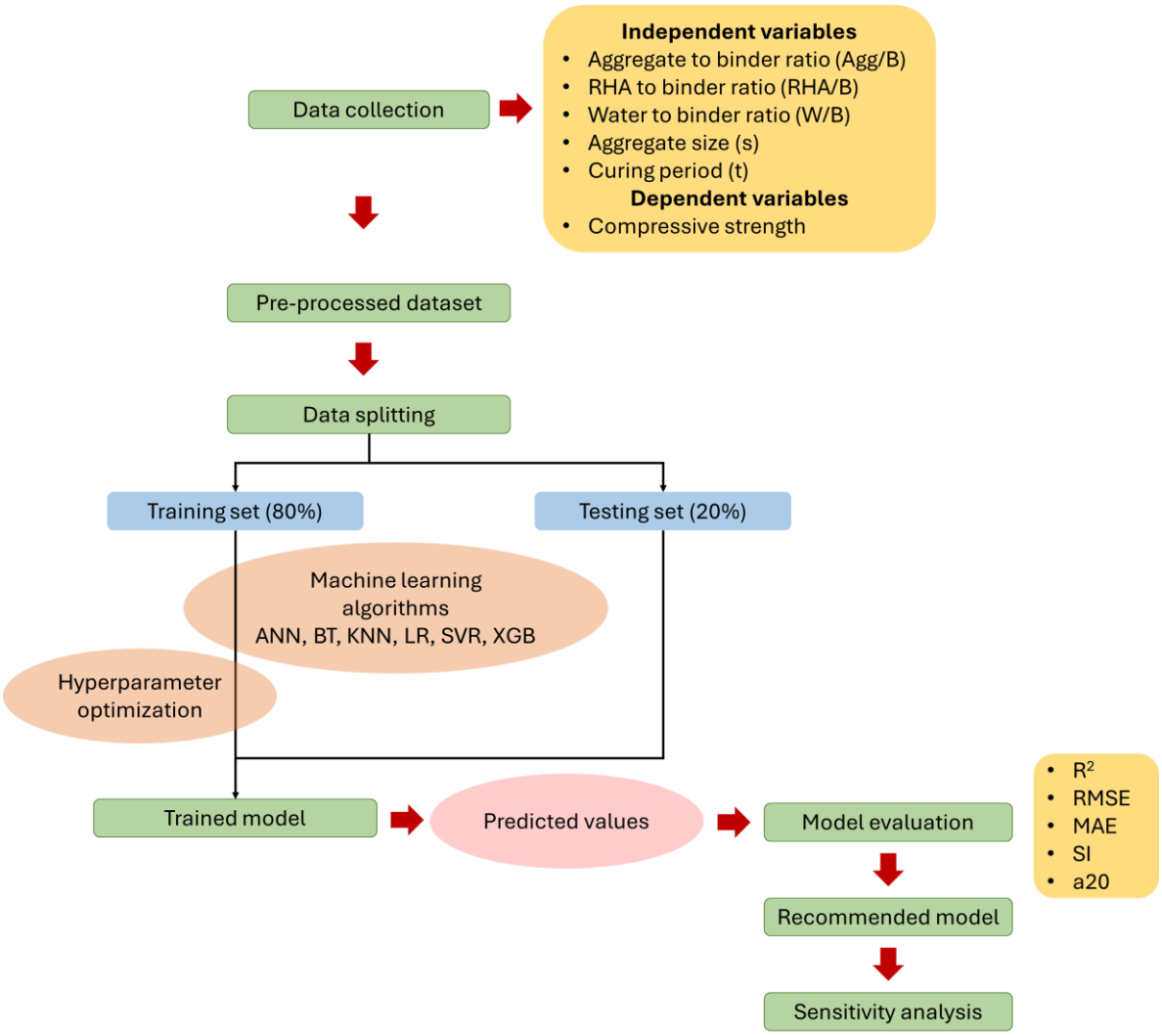

Fig. 1. ML methodology flow chart

This study employed a accurate ML approach to develop a model for forecasting pervious concrete's compressive strength, as demonstrated in **Fig. 1**. A dataset encompassing 193 data points from peer-reviewed literature served as the foundation for the analysis. Six well-established ML algorithms were investigated: Linear Regression (LR), Artificial Neural Network (ANN), Boosted Tree Regression (BT), Random Forest Regression (RF), Support Vector Regression (SVR), and Extreme Gradient Boosting (XGB).

- LR: Linear Regression is one of the simplest and most widely used statistical methods for predictive modeling. It assumes a linear relationship among independent variables (features) and dependent variable (target). LR is advantageous due to its interpretability, ease of implementation and efficiency in training. It provides a clear understanding of how each feature contributed to prediction. Despite its simplicity, LR is effective when association among features and target variable is almost linear. It serves as a baseline model in this study, allowing for comparisons against more complex algorithms.
- ANN: It is a powerful modeling technique stimulated by human brain's structure and functioning.

Composed of interconnected nodes systematized in layers, it can model complex, nonlinear associations between inputs and outputs. They are particularly effective in capturing intricate non-linear patterns in large datasets. ANNs were selected for their flexibility and capability to learn from data without explicit programming of relationships. Their ability to generalize well makes them suitable for forecasting compressive strength, where interactions among variables can be complex.

- BT: It is an ensemble ML method that merges several weak learners, usually decision trees, to form an accurate predictive model. Each tree is trained to correct errors made by preceding trees. This method is advantageous because it effectively reduces bias and variance, leading to improved accuracy. BT was selected due to its capability to handle complex nonlinear associations and connections among features, which is critical in forecasting compressive strength.
- KNN: It is a learning algorithm that does not assume any underlying data distribution. It operates by comparing instances directly, making it suitable for tasks in both classification and regression. It predicts output for a new instance by averaging the outputs of its K nearest neighbors in the training dataset. KNN is easier to recognize and instrument, making it a respectable benchmark model. It was included in this study for its capability to capture local patterns in the data, especially in cases where the association among features and target variable is non-linear.
- SVR: It extends the principles of Support Vector Machines to handle regression problems. Its objective is to identify a hyperplane that optimally represents the data while maximizing the distance between the hyperplane and the closest data points. SVR performs well in high-dimensional environments, especially when the number of dimensions surpasses the number of samples. Its robustness to overfitting, especially in high-dimensional spaces, makes it suitable for the complexities inherent in predicting compressive strength.
- XGB: It is a refined approach to gradient boosting that prioritizes efficiency and high performance. It incorporates regularization techniques to reduce overfitting and handles missing data effectively. XGB is recognized for its high predictive precision and has been widely used in various applications, including regression tasks. Its selection in this study is based on its proven performance in similar contexts and its ability to model complex interactions within the dataset.

These algorithms were chosen to deliver a comprehensive comparison of various modeling techniques, allowing for the identification of the most operative approaches for predicting compressive strength. In present study, the dataset was splitted into training and testing sets using an 80 to 20 ratio. This split was chosen to balance the need for a robust training dataset while ensuring adequate data remained for reliable performance evaluation. Hyperparameter tuning, employing a grid search technique, was implemented to optimize each model's configuration.

Additionally, five-fold cross-validation was utilized to mitigate overfitting. Model comparisons were conducted using various performance metrics, including statistical measures, a Taylor diagram, and error distribution analysis. The SHAP analysis was performed on the best-performing model to understand relative influence of independent variables on compressive strength. ML analysis utilized Python version 3.11.5 and JMP Pro v.17. JMP Pro played a primary role in hyperparameter tuning and model training. Python facilitated SHAP analysis.

2.3 Performance indicators

The performance of the proposed models was comprehensively evaluated using a differnt statistical metrics. These metrics included the R^2(coefficient of determination), RMSE (Root Mean Square Error), MAE (Mean Absolute Error), SI (Scatter Index), and a20 index (as defined in Eqs. 1-5).

$$R^2 = \left(\frac{\sum_{i=1}^{n} \left(P_i - \overline{P}\right)\left(E_i - \overline{E}\right)}{\sqrt{\sum_{i=1}^{n} \left(P_i - \overline{P}\right)^2} \sqrt{\sum_{i=1}^{n} \left(E_i - \overline{E}\right)^2}} \right)^2 \quad (1)$$

$$RMSE = \sqrt{\frac{\sum_{i=1}^{n}\left(E_i - P_i\right)^2}{N}} \tag{2}$$

$$MAE = \frac{\sum_{i=1}^{n}\left(\left|E_i - P_i\right|\right)}{N} \tag{3}$$

$$SI = \frac{RMSE}{\bar{E}} \tag{4}$$

$$a20_{index} = \frac{N_{20}}{N} \tag{5}$$

In this context, Pi denotes the forecasted strength, Ei indicates the actual strength, $\bar{P}$ represents the average of the forecasted strength, $\bar{E}$ signifies the average of the actual strengths, N is the total number of datasets, and N_{20} refers to instances where the forecasted strength is within 20% error of the actual strength.

Each metric suggestions a unique dimension on model performance, providing a comprehensive assessment of how well a model captures underlying data and align with research objectives.

- R^2: It specifies the fraction of variability in the dependent parameter which can be anticipated based on the independent parameter. Its values range from 0 to 1, with a value near 1 suggesting a superior fit of the model with the data. R^2 is critical for understanding how well a model explains variability of compressive strength predictions, allowing for comparisons between different models.
- RMSE: It is the square root of the mean of the squared differences between the forecasted and actual values. This metric reflects the extent of deviation of prediction errors from actual values, where smaller RMSE indicate improved performance of the model. RMSE is particularly useful in assessing accuracy of regression models and provides a clear empathetic of common range of prediction errors.
- MAE: It characterizes the mean of the absolute disparities among forecasted values and actual values. Unlike RMSE, which squares the errors, MAE treats all errors equally, making it easier to interpret in terms of original scale of data. MAE is beneficial in understanding average prediction error and provides an alternative measure of model accuracy that can complement RMSE.
- SI: It is a normalized measure of prediction accuracy, calculated as the ratio of RMSE to the mean of observed values. It offers a unitless metric for assessing model performance, facilitating straightforward comparisons across various datasets. SI values can be taken as follows: $SI > 0.3$: Poor e, $0.2 < SI \leq 0.3$: Acceptable, $0.1 < SI \leq 0.2$: Excellent, $0 \leq SI \leq 0.1$: Great performance.
- a20 Index: It measures the percentage of forecasted strength that lie within a defined range (20%) of the actual strength. This is determined by splitting the count of forecasts within that range by the total number of data. This metric is especially valuable for evaluating the real-world relevance of models, as it shows how frequently the predictions are reasonably close to the actual measurements.

2.4 Hyperparameter tuning

In this study, hyperparameter optimization was a critical step to enhance performance of ML models. A grid search was employed for hyperparameter tuning, which methodically investigates a predefined values of hyperparameter to categorize a combination that produces the best model performance. This method assesses all probable combinations of specified hyperparameter values, allowing for a comprehensive assessment of their impact. Each ML algorithm has specific hyperparameters that influence its performance. For instance, the ANN involved tuning the number of layers and number of nodes per layer, while KNN required selecting the optimal number of neighbors (k). The BT model was optimized by adjusting number of layers and number of splits per tree, whereas

SVR involved tuning the kernel type, cost, and gamma parameters. For XGB, hyperparameters such as max depth, subsample, colsample by tree, min child weight, learning rate, and iterations were fine-tuned. Performance of each hyperparameter configuration was assessed using R^2 and RMSE as primary metrics, with the aim of maximizing R^2 and minimizing RMSE. To ensure robust evaluation and mitigate overfitting, five-fold cross-validation was applied during optimization process, dividing the training dataset into five equally sized folds. This comprehensive approach to hyperparameter optimization intended to find the most effective configurations for each ML algorithm, ultimately enhancing the forecasting accuracy of the models for compressive strength.

3. Results and discussion

3.1 Effect of RHA on compressive strength

This study investigates the consequence of RHA substitution level on strength. Findings suggest an optimal RHA content for achieving maximum strength. Previous research has shown a trend where compressive strength generally increases with RHA addition up to a certain point, followed by a decrease beyond that point. This phenomenon is evident in **Fig. 2(a)**, where compressive strength steadily rises until a 10% RHA replacement level and then declines with further RHA incorporation.

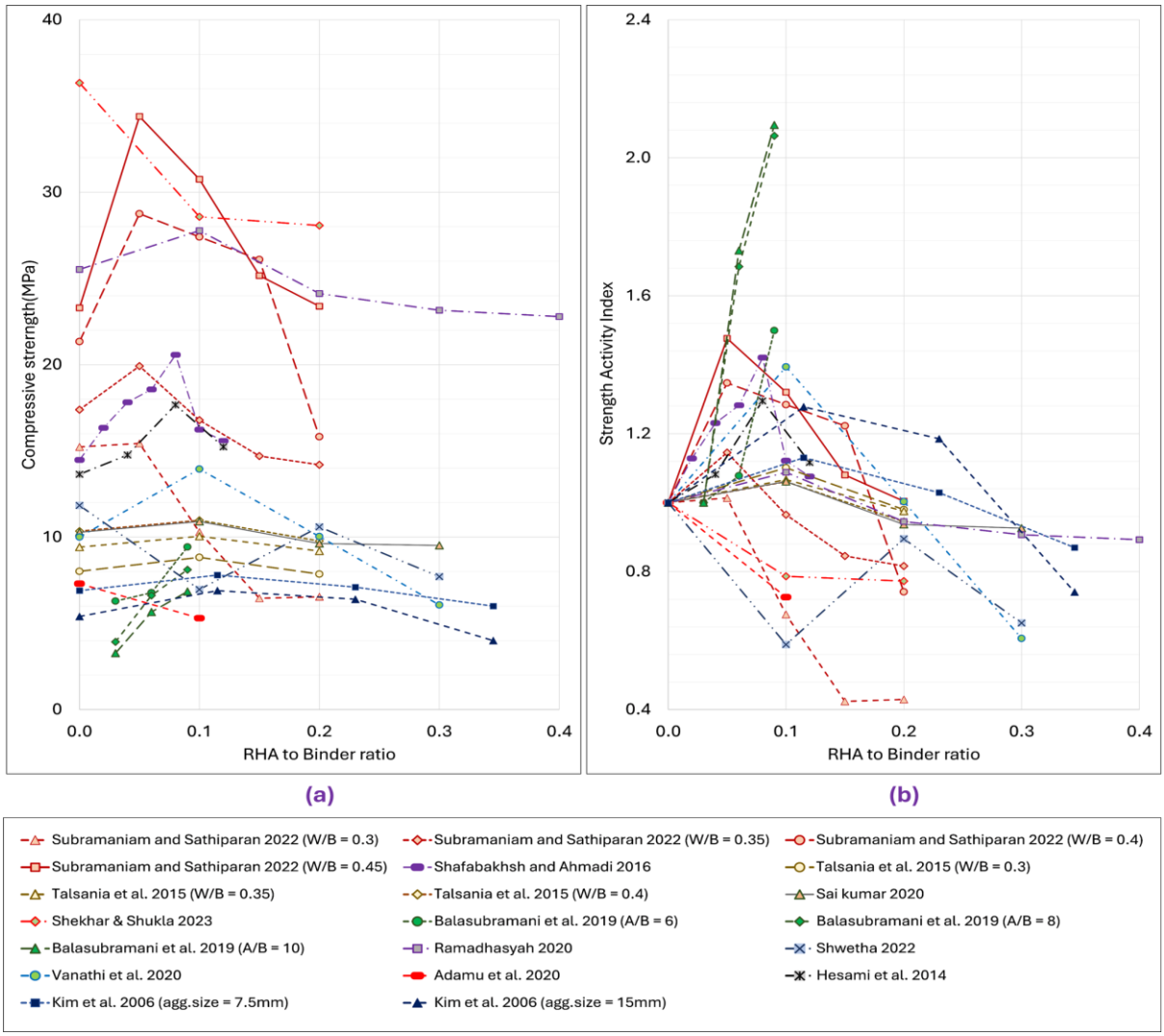

Fig. 2. (a) compressive strength and (b) strength activity index variation with RHA to binder ratio

Initial strength gain can be attributed to RHA's pozzolanic nature. RHA reacts with calcium hydroxide during cement hydration, forming additional cementitious gel that increase concrete strength. However, excessive RHA content can introduce higher porosity due to its finer particle size than cement.

This increased porosity disrupts the formation of a strong and continuous network within the concrete, ultimately reducing compressive strength.

Fig. 2(b) explores the strength activity index (SAI) changes with increasing RHA/B ratio. SAI is a relative measure of the compressive strength between RHA-blended and control pervious concrete. Equation (6) expresses the observed trend in the SAI with R^2= 0.0971:

$$SAI = 1 + 1.4544\left(RHA/B\right) - 6.6993\left(RHA/B\right)^2 \quad (6)$$

Analysis indicates that maximum strength, on average, is achieved at a 9% RHA replacement level. At this optimal level, the ultimate strength achieved is 8% higher than the control pervious concrete. This equation's correlation coefficient (R^2) is 0.0971, indicating a weak relationship between the RHA/B ratio and the SAI. This suggests that other mix parameters likely influence compressive strength of RHA blended pervious concrete.

3.2 Statistical analysis

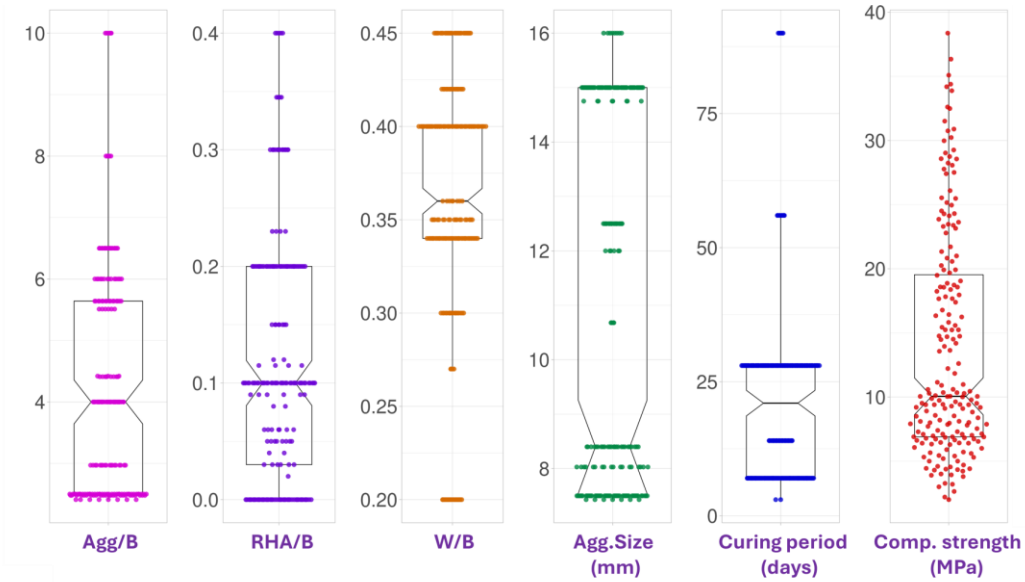

	Agg/B	RHA/B	W/B	Agg.Size (mm)	Curing period (days)	Comp. strength (MPa)
Mean	4.20	0.12	0.36	11.00	21.19	13.81
Min.	2.41	0.00	0.20	7.43	3.00	2.00
Max.	10.00	0.40	0.45	16.00	90.00	38.37
Std	1.91	0.10	0.07	3.38	16.82	8.74
Skewness	1.07	0.77	-0.92	0.22	1.99	0.87
Kurtosis	0.69	-0.06	0.46	-1.78	5.51	-0.29

Fig. 3. Data distribution of independent and dependent variables

Fig. 3 characterizes the distribution of variables. Statistical analysis was conducted and their values are documented within the figures for each variable. These statistics deliver valuable understandings into the data distribution. Notably, all parameters except W/B ratio exhibited positive skewness. This observation suggests positive skewness in the spreading, with a tail spreading to higher values. Significantly positive kurtosis values for Agg/B, W/B, and curing period suggest that these variables are leptokurtic. In contrast, a negative kurtosis value for the aggregate size and compressive strength suggests that these parameters have shorter tails than a normal distribution. This suggests that there are fewer extreme values than typically anticipated in a normal distribution.

Statistical analysis investigated relationships between selected parameters and compressive strength. Results in **Fig. 4** indicate that Agg/B, aggregate size, and curing period have higher correlation with compressive strength. It's important to note that no correlations were observed between independent parameters, except for Agg/B and aggregate size. Curing period exhibited the strongest positive correlation (R = 0.46) with strength, followed by the W/B ratio (R = 0.18). Conversely, increasing Agg/B ratio (R = -0.62) and aggregate size (R = -0.62) negatively correlated with compressive strength.

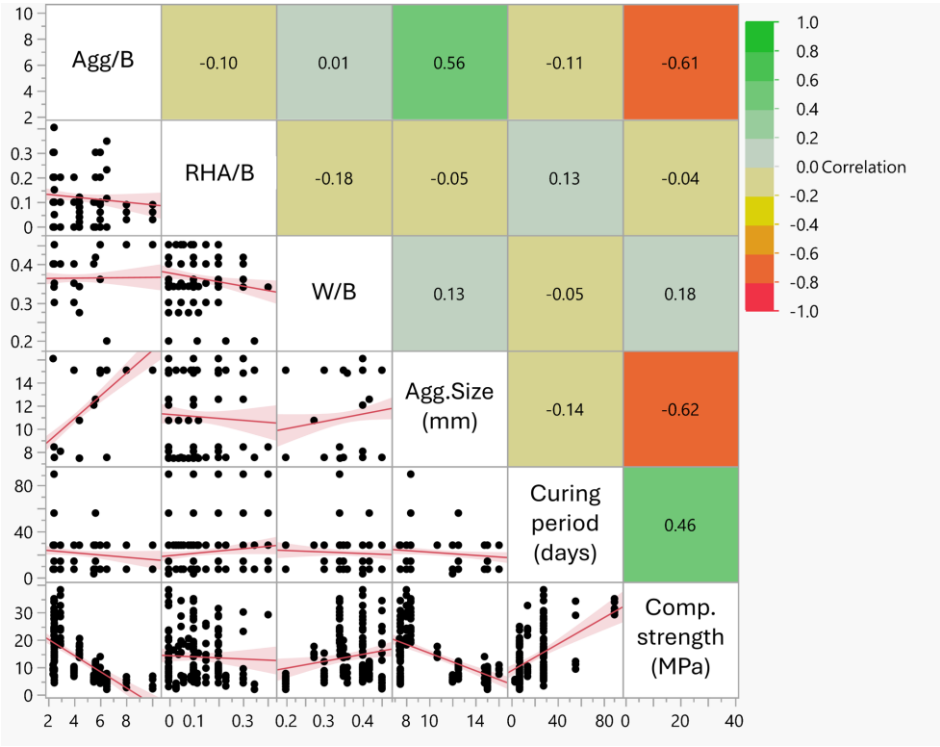

Fig. 4. Correlation between variables

Size of aggregates significantly influenced compressive strength of pervious concrete. Larger aggregates tend to create larger voids within concrete matrix, which can negatively affect overall strength by reducing the effective area available for load transfer. Research has shown that smaller aggregate sizes can lead to a denser packing of particles, enhancing interlocking and stability of concrete structure [14]. In contrast, when larger aggregates are used, increased porosity may result in a weaker matrix, as interlocking between particles is compromised [46]. This phenomenon is supported by studies indicating that strength reductions with larger aggregate size [47]. Furthermore, it is essential to consider aggregate grading; well-graded aggregates can optimize packing density and minimize voids, thereby enhancing strength of the concrete [12]. These findings suggest that careful consideration of aggregate size and grading is crucial to achieve anticipated compressive strength in pervious concrete.

3.3 Hyperparameters optimization

Six comprehensive algorithms were implemented during the ML model training process. A detailed account of the hyperparameters utilized in this study is provided in **Table 3**. A grid search method was employed to optimize prediction performance for hyperparameter tuning. While methods like random search and Bayesian optimization are also effective, grid search allows for a thorough evaluation of specified parameter combinations, ensuring that we capture the intricacies of the model's performance across various settings. This approach is particularly beneficial when number of hyperparameters is relatively small, as it provides a comprehensive understanding of their impact on model accuracy.

Cross-validation is a critical statistical method for evaluating and assessing the performance of ML models. Assessing chosen models' performance is critical. Validation techniques are necessary to evaluate a model's data accuracy. Consequently, five-fold validation was adopted to moderate overfitting and bolster robustness of ML models. Prior research has extensively documented the advantages of employing a 5-fold cross-validation approach, as it demonstrably yields favorable time-based outcomes [48]. Five-fold cross-validation approach was employed for model evaluation. Dataset was divided into five equally sized folds. In each iteration of the five-fold cross-validation, four folds were utilized for training the model, and the remaining fold was used for validation. This ensured that each fold served as the validation set once. This process mentioned above was meticulously repeated five times to guarantee thorough testing.

Table 3. Hyperparameters used for the ML models

Model	Hyperparameters	Selected value	Analyzed Values
ANN	Number of layers	2	[1, 2]
	Nodes per layer	[8, 8]	[1-10]
KNN	k	2	[1-10]
BT	Number of layers	5	[1-10]
	Split per tree	10	[1-10]
	Learning rate	0.5	[0.01, 0.1, 0.25, 0.5, 1]
SVR	Kernel	Radial basis function	[linear, Radial basis function]
	Cost	4.97785	[0.01-5]
	Gamma	0.49884	[0.001-0.5]
XGB	Max_depth	5	[1-5]
	Subsample	0.6088	[0.5-1]
	Colsample_by tree	0.8228	[0.5-1]
	Min_child_weight	1.3704	[1-3]
	Alpha	0.0832	[0-0.5]
	Lambda	0.0131	[0-2]
	Learning rate	0.1867	[0.05-0.2]
	Iterations	16	[0-20]

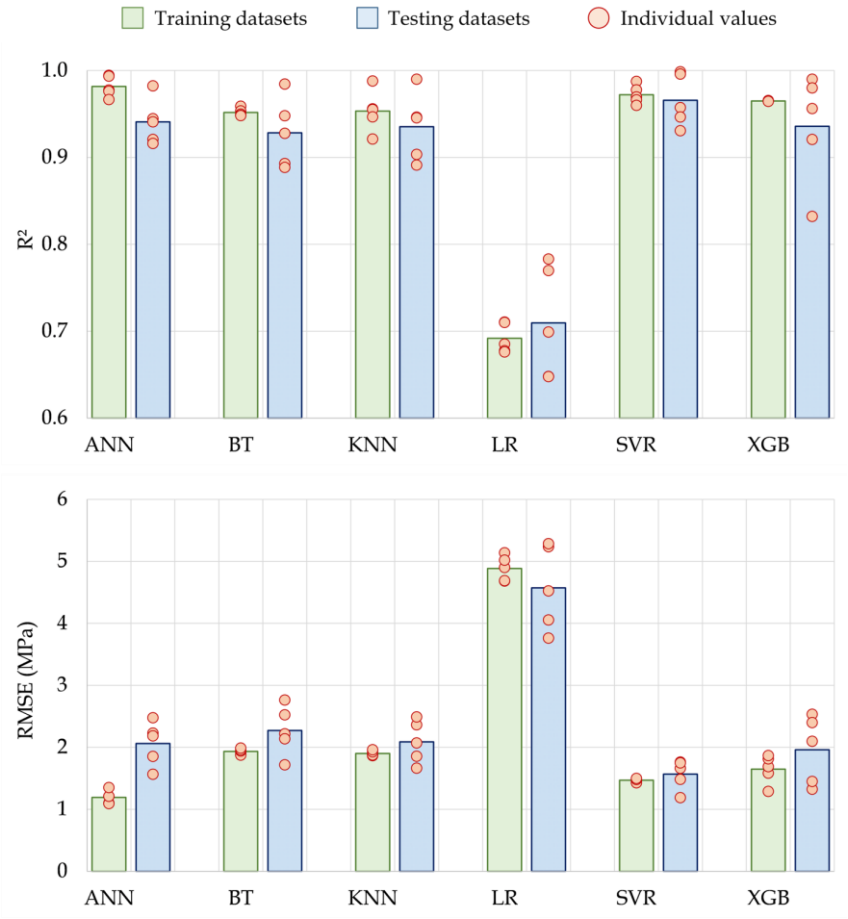

Fig. 5. Performance indicators for k-fold validation

Outcomes of K-fold cross-validation is showed in **Fig. 5**. For training dataset, ANN exhibited superior R^2 and smaller RMSE than other ML models. However, the SVR model demonstrated superior performance for the validation dataset. Notably, ANN and SVR models achieved R^2 values surpassing 0.97 for all training dataset folds. For training dataset, each model displayed a limited range of discrepancy in R^2. Conversely, for validation datasets, only ANN and SVR models exhibited a contracted range of variation in R^2 (discrepancy of maximum and minimum R^2), which was

approximately 0.07. The XGB model displayed a significant variation in R^2 for validation datasets. This tendency was similarly detected for RMSE values. ANN and SVR models revealed excellent performance in training and testing datasets. SVR revealed narrowest range of RMSE values, varying between 1.43 MPa to 1.50 MPa for training datasets and 1.19 MPa to 1.76 MPa for validation datasets, respectively. The aforementioned findings imply that ANN and SVR models are not susceptible to overfitting and more reliable ML models for prediction.

3.4 Models' performance

While a model's performance is evaluated using the dataset compiled, it is essential to note that k-fold cross-validation techniques were employed to mitigate risk of overfitting. This method divides the dataset into multiple subsets, allowing a model to be trained on different combinations of data fractions and validated on unseen portions, thus providing a more robust assessment of its accuracy.

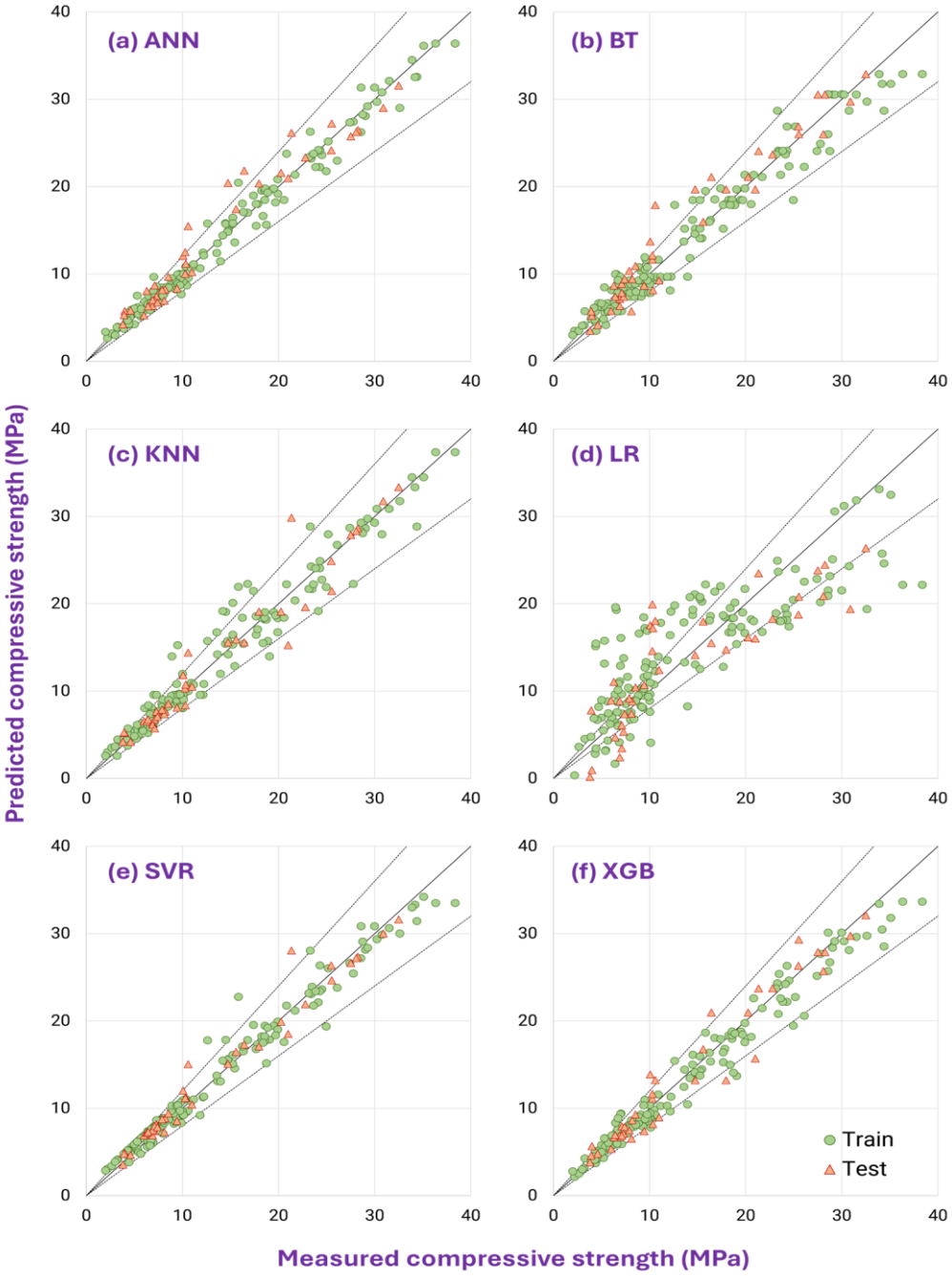

Fig. 6. Predicted vs. actual strength for different ML algorithms

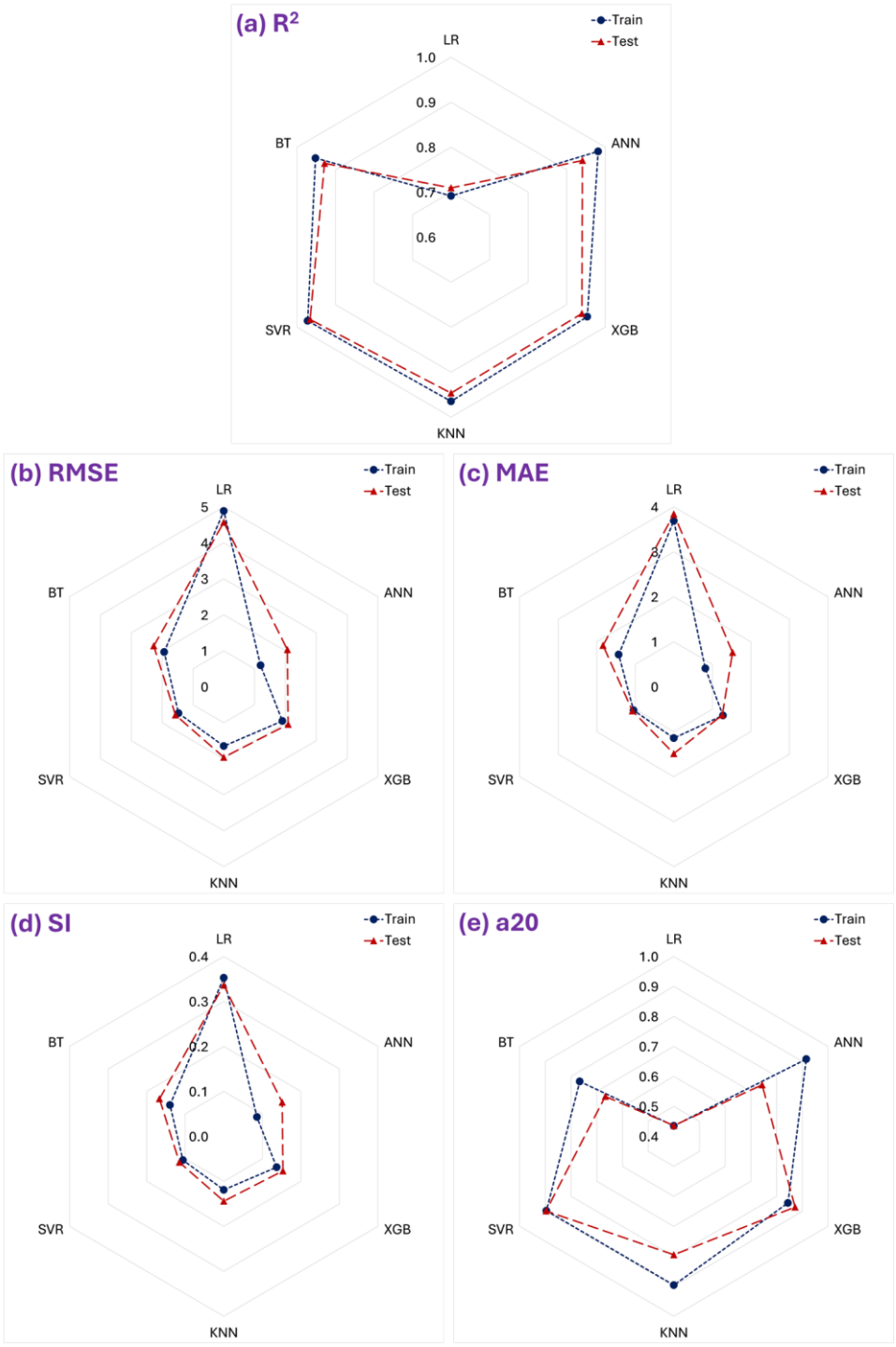

Fig. 7. Performance index variation for different ML algorithms

Among the models evaluated (**Fig. 6** and **Fig. 7**), the SVR model demonstrated the most robust predictive capabilities. This conclusion is substantiated by the SVR model's significantly higher R^2 related to other models. Furthermore, the SVR model showed notably lower RMSE and MAE, demonstrating a high degree of accuracy in aligning estimates with observed data. While the ANN model confirmed greater performance on the training dataset, its generalization ability, as evidenced by its performance on the testing dataset, was outperformed by the SVR model. Further validation using the SI value and a20 index verified the SVR model's accuracy. The SVR model exhibited a lower SI value, signifying its effectiveness in minimalizing the discrepancy among predicted and measured values. Notably, the SI values for both training and testing datasets (0.11 and 0.12, respectively)

highlight the model's consistent performance across known and unseen data. Moreover, the analysis revealed that 90% of predicted values for both datasets fell within a 20% error margin of the measured values.

The combined results clearly express the greater performance of the SVR model. Related to other models, the SVR model exhibited a higher R^2 and smaller values for RMSE, MAE and SI. Furthermore, a smaller a20 index further supports its strong generalization capabilities. These findings strongly suggest that the SVR model effectively captures the intricate relationships and complications inherent within the data. This interprets to exceptional forecasting accuracy, crafting it a highly valued tool for forecasting applications. The model's accuracy and consistency underscore its significant potential to subsidize meaningfully to the field of predictive analytics.

A comprehensive analysis of ML models reveals that SVR model outperformed other algorithms in forecasting compressive strength. Superior performance of SVR can be attributed to its capability to efficiently handle high-dimensional data and capture complex, nonlinear relations among input features and target variable. By maximizing the margin between predicted values and actual data points, SVR minimizes prediction errors and enhances generalization capabilities, making it particularly robust against overfitting. In contrast, while ANN model demonstrated strong performance, its complexity can lead to overfitting, especially with smaller datasets. ANNs require careful tuning of hyperparameters and sufficient training data to achieve optimal results. Although they are highly flexible and capable of modeling intricate relationships, their lack of interpretability can be a limitation when attempting to understand the underlying factors affecting predictions.

BT algorithm also showed competitive results, benefiting from its ensemble learning approach that combines multiple weak learners. However, it may require significant computational resources and can be sensitive to noisy data, which may affect its performance in certain scenarios. Similar to ANN, BT models can be prone to overfitting if not properly regularized. KNN offered a simple yet effective method for prediction, but its performance is vastly reliant on the select of 'k' and the distance metric utilized. While KNN can capture local patterns, it tends to struggle with high-dimensional data due to "curse of dimensionality," leading to decreased accuracy as the number of features increases. XGB is recognized for predictive power and competence; however, it can be complicated to tune due to numerous hyperparameters. XGB excels in handling missing values and modeling complex interactions, but its performance may vary significantly with different datasets, necessitating careful validation.

3.5 Taylor diagram

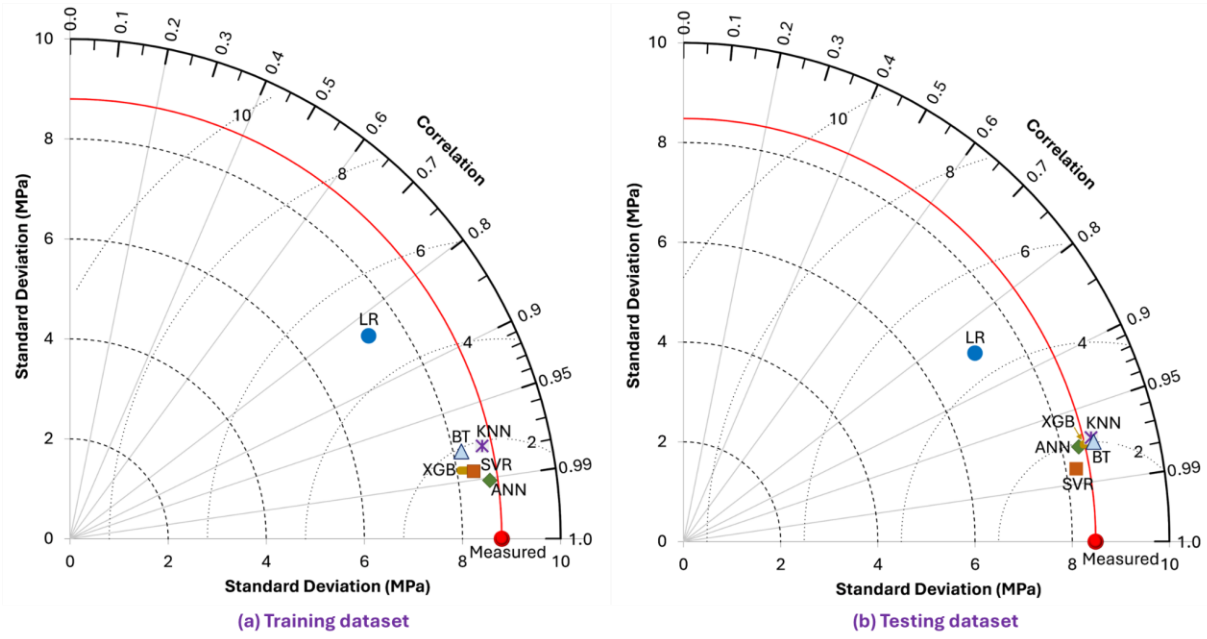

Fig. 8. Taylor diagram for performance of ML models

A Taylor diagram was utilized to evaluate performance of ML models in prediction. Proximity of a model's marker to reference point (depicted by a red line in **Fig. 8**) reflects the agreement between its predictions and measured compressive strength values. This agreement is quantified by considering fundamental statistical properties such as standard deviation and correlation coefficient. Among evaluated models, ANN exhibited the closest correspondence to reference point for the training dataset, followed by SVR and XGB models. Conversely, LR model displayed the furthest distance from reference point in training and testing datasets, indicating significant deviations between its predictions and actual data. Taylor diagram also incorporates a horizontal line representing correlation between forecasted and actual strength. The SVR model's proximity to this line indicates a stronger correlation compared to the other models.

3.6 Error distribution

Fig. 9 shows the error distribution for several ML models employed to forecast compressive strength, where error is defined as the discrepancy between forecasted and measured values. The illustration offers important perceptions into the predictive capabilities of models. The LR shows a considerable presence of outliers, with data points that significantly stray from the average trend. This indicates a possible drawback of the LR model in adequately representing the complex relationships in the data. In contrast, the ANN model shows the highest level of consistent predictive accuracy among the models assessed. This is reflected in a tighter error range, from -3.61 to 5.67 MPa, suggesting a smaller gap between the forecasted and actual compressive strength values.

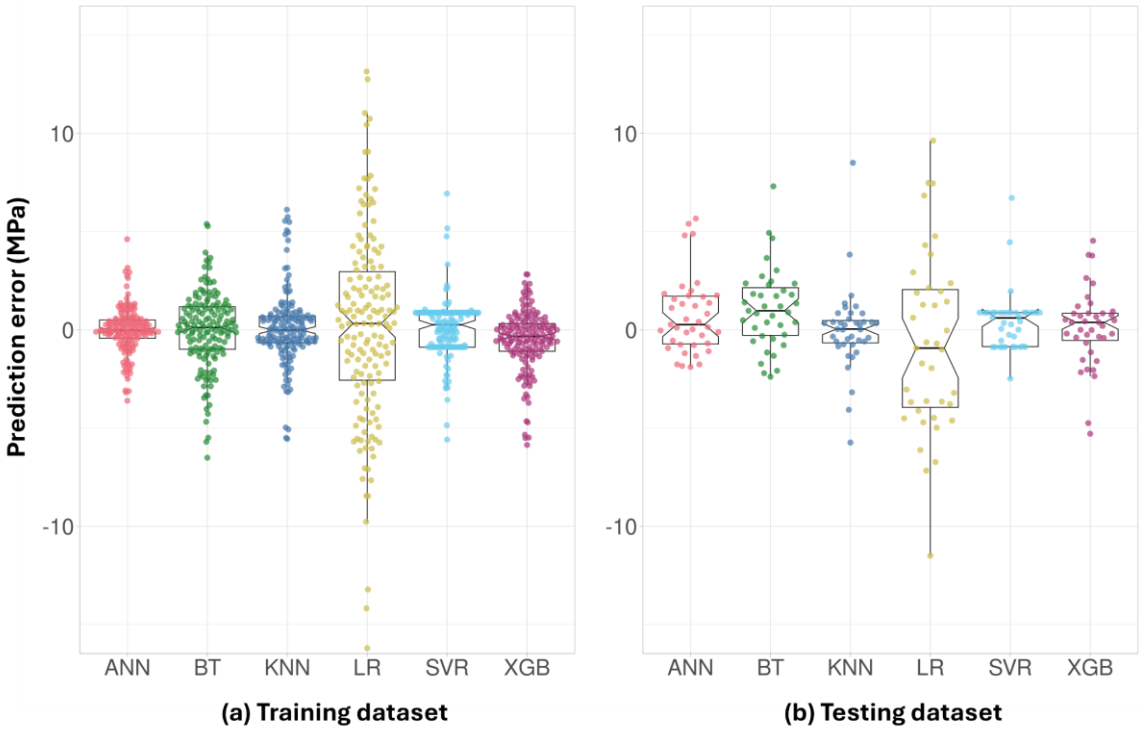

Fig. 9. Error distribution for various ML algorithms (a) training dataset and (b) testing dataset

ANN, KNN, and SVR model error distributions exhibit positive skewness. This specifies that mean error is higher than median error. Besides, all three models have a positive average error, indicating a consistent underestimation of compressive strength. In contrast, XGB and BT models display negative skewness. While BT model exhibits negative skewness, its average error value remains positive (+0.22 MPa). This suggests a few higher errors on the negative side, potentially outweighing overall distribution towards underestimation. These observations underscore the necessity of utilizing a broad array of statistical metrics and visualizations, in addition to mere visual assessment, to thoroughly assess the performance of prediction models. This comprehensive approach offers a deeper insight into the strengths and weaknesses of each model.

Fig. 10 illustrates production errors associated with various ML models across different compressive strength ranges. For strengths below 8 MPa, all models tend to overestimate predictions. SVR model exhibits a narrow error distribution, followed closely by the XGB model. In strength range of 8 to 16 MPa, error distribution is fairly balanced around zero, though several instances show a higher positive error. XGB model again demonstrates a narrow error distribution, while SVR model's prediction errors are predominantly closer to zero, with a few outliers. For strengths exceeding 16 MPa, all ML models tend to underestimate predictions. XGB model continues to show a narrow error distribution, followed by ANN and SVR model.

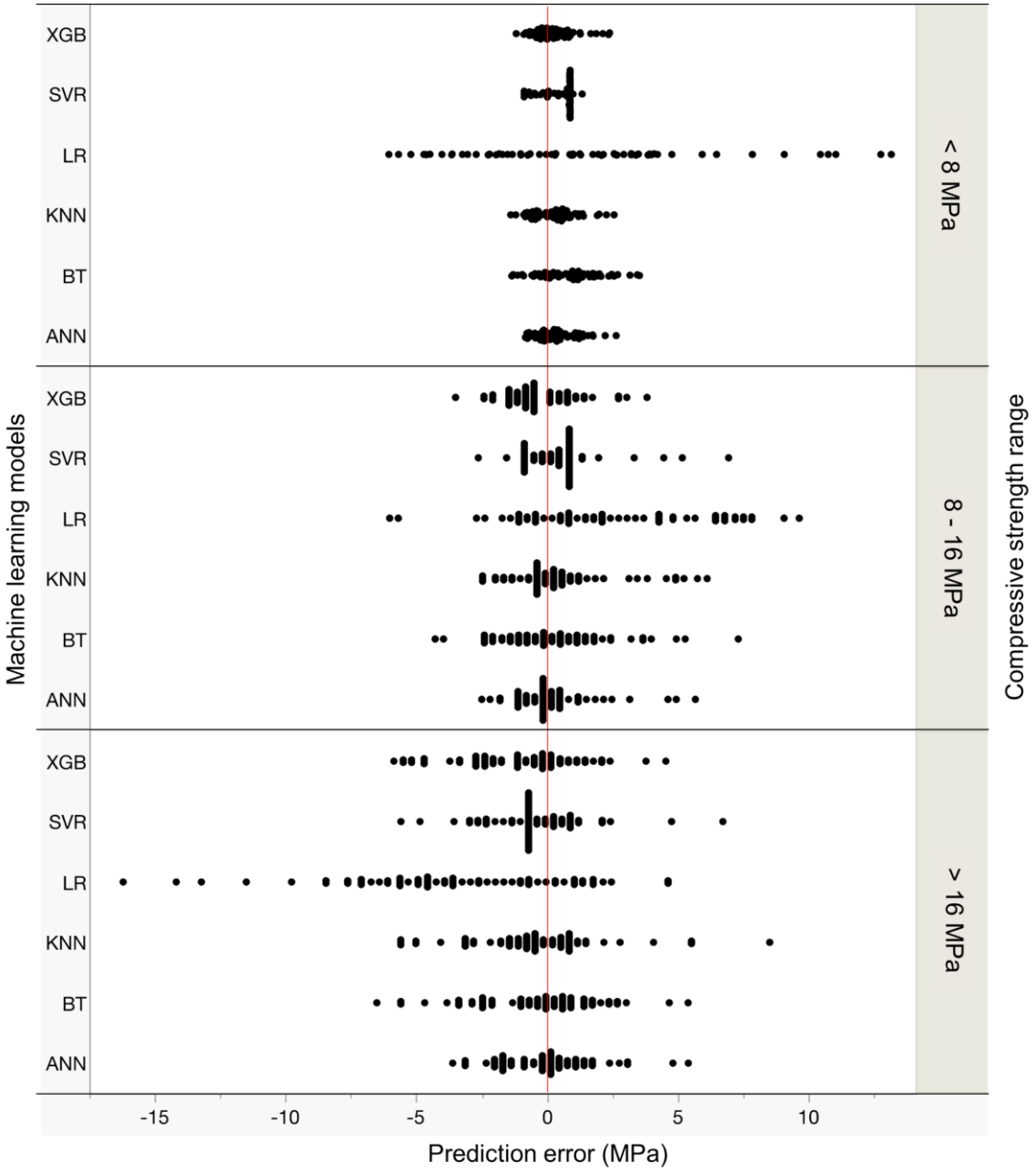

Fig. 10. Error distribution for various ML algorithms and compressive strength range

3.7 Sensitivity analysis

SHAP (SHapley Additive exPlanations) is a method utilized in ML to explain individual predictions made by a model. SHAP values are a powerful tool for interpreting predictions of ML models, providing insights into contribution of each feature to final prediction. By applying cooperative

game theory principles, SHAP values assign each feature an importance score based on its marginal influence to the prediction, allowing for a clear understanding of how different variables influence a model's outputs. In this study, SHAP values were computed for top-performing models, particularly focusing on Support Vector Regression (SVR) model [49]. SHAP defines the influence of each parameter to the model's prediction in relation to a baseline prediction. This enables understanding of how each feature influences the prediction towards the final outcome. SHAP offers various ways to visualize these feature contributions, including force, summary, and dependence plots. These visualizations help interpret the influence of each parameter on model's output [50].

Mean SHAP values provided in **Fig. 11** indicate the feature contributions to predicting compressive strength of RHA blended pervious concrete. Higher SHAP values represent a more significant impact on model's predictions. Aggregate size has the most substantial positive effect (SHAP value = +4.81) on compressive strength in this analysis. W/B ratio (+2.25) and Curing Period (+2.19) also have significant positive influences. Agg/B ratio (+1.41) and RHA/B ratio (+1.09) also have positive effects but to a lesser extent than previous factors. An optimal balance between Agg/B is crucial, and including RHA can contribute to strength enhancement, but likely through mechanisms like pore refinement or pozzolanic reaction.

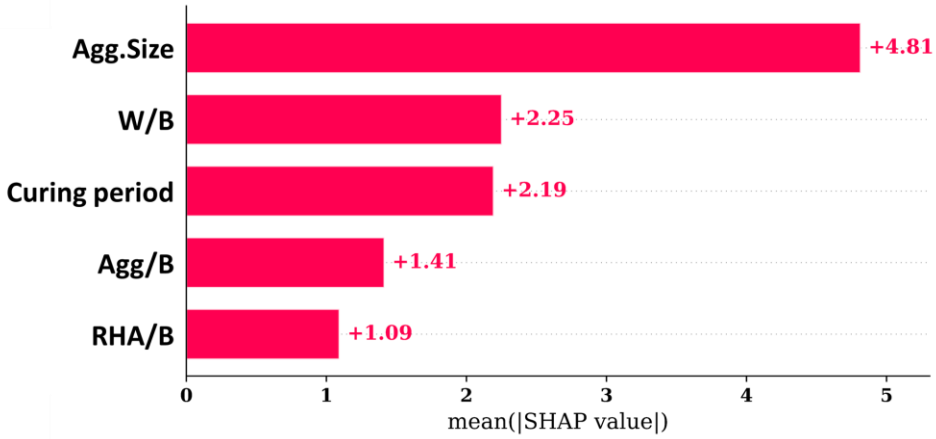

Fig. 11. Mean SHAP values for the model

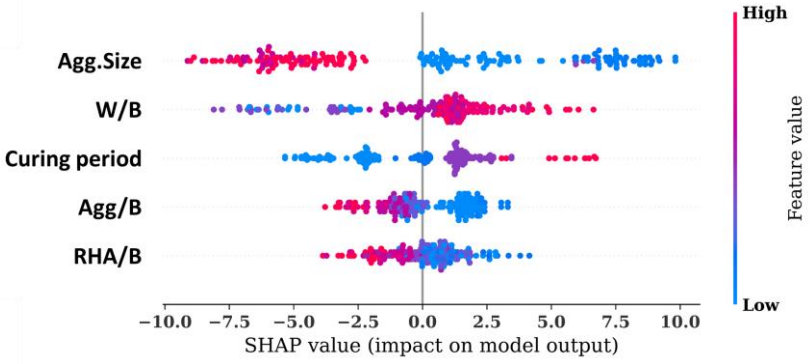

Fig. 12. SHAP summary plot for the model

SHAP summary plots in **Fig. 12** illustrate influences of specific parameter to model's compressive strength estimation. Colour gradient along x-axis characterizes the range of values for each parameter. Position of a data point on y-axis indicates raw feature value itself. Red dots specify parameter with high values associated with robust positive SHAP values. Notably, a substantial positive SHAP score of 10 is recorded for lower aggregate size. This finding recommends that within the investigated range, smaller aggregates can enhance predicted compressive strength by 10 MPa compared to an average value. A negative SHAP value of -10 at the far left of x-axis specifies that larger aggregates may reduce predicted compressive strength by 10 MPa comparative to average. Pervious concrete relies on interlocking of aggregate particles for strength. Larger aggregates leave bigger voids between them, hindering this interlocking effect and leading to a weaker matrix. Also, larger aggregates contribute to

a higher overall void content in the concrete mix [46]. This porosity reduces effective load-bearing area, translating to lower compressive strength. During compression testing, larger aggregates are more prone to crushing under pressure within the porous structure, compromising the concrete's strength.

This study establishes a positive correlation among curing time and compressive strength as a higher W/B ratio and a more extended curing period positively influence compressive strength. Extended curing periods enhance compressive strength due to facilitation of cement hydration. Hydration is a chemical reaction between water and cement, forming hydration products that contribute to strength. A longer curing duration allows a more complete hydration process, ultimately leading to a higher compressive strength [51]. It is shown that lower Agg/B ratio positively affects compressive strength. Agg/B directly influences the mortar matrix's density and particle packing. A higher ratio signifies a reduction in cementitious material available to bind aggregate particles, consequently hindering compressive strength development. While the impact of RHA on compressive strength is less pronounced compared to other parameters, it still exerts a significant influence. In general, mortars formulated with higher RHA/B ratios exhibit lower compressive strength.

3.8 Comparison with past studies

Table 4. Overview of the ML model for estimating compressive strength of SCMs-enhanced pervious concrete

Ref	SCMs used [1]	Impendent variable [2]	Data points	MLs used	R^2 (Train)	RMSE (Train)	R^2 (Test)	RMSE (Test)	Best model
Yu et al. [24]	Fly ash, Silica fume	C.C, C.Agg, F.Agg, W, SCM, Admix	123	CNN BPNN	0.94	2.72 4.07	0.94	3.00 3.31	CNN
Sathiparan et al. [23]	Fly ash	Agg/B, W/B, SCM/B, Agg.S, t	437	ANN BT LR RF SVR XGB	0.82 0.96 0.40 0.92 0.71 0.99	4.21 2.07 7.67 2.89 5.13 0.86	0.82 0.92 0.42 0.89 0.71 0.95	4.58 3.09 8.31 3.57 5.73 2.53	XGB
Sathiparan et al. [25]	Silica fume	C.C, SCM, C.Agg, F.Agg, W, Admix, Agg.S, t	222	ANN BT KNN LR RF SVR XGB	0.95 0.93 0.85 0.44 0.95 0.91 1.00	2.71 3.20 4.74 9.17 2.86 3.63 0.28	0.94 0.87 0.86 0.42 0.90 0.85 0..97	3.05 4.32 4.59 9.30 3.87 4.72 2.21	XGB
Sudhir Kumar et al. [21]	GGBS	C.C, SCM, Agg.S, Porosity	18	ANN	0.99	0.12	0.99	0.14	ANN
Ahmad et al. [22]	Waste glass powder	C.C, SCM, W/B, C.Agg, t	99	LR NLR ANN	0.77 0.82 0.99	2.72 2.39 0.53	0.79 0.89 0.99	2.72 1.37 0.49	ANN
Sathiparan et al. [16]	Metakaolin	Agg/B, W/B, SCM/B, Agg.S, t	131	ANN BT RF XGB	0.96 0.97 0.99 0.98	1.49 0.86 0.18 0.19	0.96 0.97 0.95 0.96	2.05 1.85 2.13 1.95	XGB
Le et al. [26]	Silica fume	Agg/B, SCM/B, W/B, F.Agg, Agg.S	164	XGB RF SVR ANN	0.98 0.97 0.97 0.93	1.44 1.58 3.75 2.56	0.92 0.90 0.89 0.88	3.38 3.61 3.72 3.81	XGB
Present study	RHA	Agg/B, W/B, SCM/B, Agg.S, t	193	ANN BT KNN LR SVR XGB	0.98 0.95 0.95 0.69 0.97 0.96	1.19 1.93 1.90 4.89 1.47 1.65	0.94 0.93 0.94 0.71 0.97 0.95	2.06 2.27 2.09 4.57 1.57 1.96	SVR

[1] GGBS: Ground Granulated Blast-furnace Slag

[2] Agg/B: Aggregate to binder ratio, Admix: Admixture content (in kg/m^3), C.C: Cement content (in kg/m^3), C.Agg: Coarse aggregate content (in kg/m^3), F.Agg: Fine aggregate content (in kg/m^3), SCM: Supplementary cement material content (in kg/m^3), SCM/B: Supplementary cement material content to binder ratio, W/B: Water to binder ratio, Agg.S: Mean coarse aggregate size (mm), t : Curing period (days)

Reviewing existing research summarized in **Table 4**, we can see a focus on mixed design parameters as input variables for ML models predicting compressive strength of pervious concrete blended with SCMs. These studies commonly used input variables include:

- Mix Proportions: Agg/B ratio (or cement and aggregate content), SCM-to-binder ratio (or SCM content), and W/B ratio (or water content).
- Material Properties: Aggregate size.
- Curing Conditions: Curing period.

Several studies highlight the effectiveness of specific models. Sathiparan et al. [16, 23, 25] and Le et al. [26] demonstrate the high accuracy of XGB models for predicting compressive strength. Kumar et al. [21] and Ahmad et al. [22] advocate for ANN, but their evaluations lack a comparison with other machine-learning approaches. This current research demonstrates comparable accuracy of SVR, ANN, and XGB models. However, limited datasets are a fundamental limitation identified across existing studies. Future research efforts should prioritize the expansion of datasets to enhance model performance and generalizability further.

This study builds upon existing research on pervious concrete by specifically investigating effect of RHA on compressive strength and employing ML techniques for predictive modeling. While previous studies have explored various SCMs such as silica fume and fly ash, this research distinguishes itself by focusing on RHA, an agricultural waste product that presents both environmental and economic advantages. Unlike earlier works that primarily utilized traditional methods for strength prediction, this study leverages advanced ML algorithms, including SVR, to provide a more accurate and nuanced empathetic of the relationships among mix design parameters and compressive strength. The application of SHAP analysis in this context is another novel aspect, offering insights into feature importance and the specific contributions of various parameters to the model's predictions. By highlighting the optimal RHA replacement level for compressive strength and demonstrating the forecasting competences of ML models, this research contributes valuable knowledge that can promote eco-friendly building methods.

4. Conclusion

This study examined the effect of RHA on compressive strength of pervious concrete and explored the use of ML models to predict this strength. The analysis leads to the following conclusions.

- A positive correlation is observed between RHA content and compressive strength up to a specific point. The optimal RHA substitute level for achieving maximum strength was found to be around 10%. At this optimal level, pervious concrete containing RHA exhibited an 8% improvement in compressive strength compared to control concrete without RHA. Beyond the 10% replacement level, incorporating more RHA caused in a reduction in compressive strength.

- Among investigated ML algorithms, the SVR model appeared as the most efficient for forecasting compressive strength. SVR model demonstrated superior performance, achieving a high coefficient of determination (R^2) of over 0.97, indicating a robust correlation among forecasted and actual strength. Furthermore, the SVR model exhibited smaller RMSE and MAE values, signifying better accuracy in its predictions. These low error values suggest minimal deviations between predicted and actual compressive strength.

- Hyperparameter optimization played a critical role in improving predictive performance of ML models. Through grid search techniques and cross-validation, the authors fine-tuned hyperparameters for each model, leading to improved accuracy and reduced risk of overfitting. The optimized parameters for SVR model, for instance, contributed significantly to its ability to capture the underlying relationships in the dataset.

- SHAP analysis showed that aggregate size is a significant factor affecting the compressive, followed by the binder ratio and curing period.

4.1 Future Research Directions

Looking forward, future research could explore several avenues to enhance understanding and application of RHA in pervious concrete. Investigating durability of RHA-blended pervious concrete under variable environmental circumstances would provide essential insights into its practical applications. Additionally, developing the dataset to comprise more diverse sources of RHA and varying mix designs could improve predictive models' accuracy and generalizability. Further studies could also examine the effects of combining RHA with other SCMs, potentially leading to innovative formulations that optimize both performance and sustainability. Lastly, exploring mechanistic pathways of how RHA interacts with other components in concrete mix through advanced analytical techniques could deepen the understanding of its pozzolanic activity and overall impact on concrete properties. Future research could consider incorporating following data sources and parameters into ML models:

- Local environmental circumstances: Data such as humidity, temperature, and precipitation in curing process can significantly influence hydration of concrete. Including these variables may help in understanding their impact on compressive strength.
- Chemical composition of RHA: Analyzing chemical properties of RHA, such as silica content and pozzolanic activity, could provide insights into how variations in RHA quality affect concrete performance.
- Particle size distribution: Detailed information on particle size distribution of both RHA and aggregates could enhance the model's capability to forecast strength by accounting for variations in packing density and inter-particle bonding.
- Long-term curing effects: Data from long-term studies on compressive strength development over time could improve predictions by allowing models to factor in time-dependent behaviors.
- Mix design variations: Comprising a broader range of mix design parameters, including different types of aggregates or additional supplementary cementitious materials (SCMs), could provide a more comprehensive dataset for training the models.

Incorporating these data sources could lead to more accurate and robust predictions, ultimately aiding engineers in optimizing concrete mixes for specific applications. The insights gained from this study can directly inform construction practice, guiding engineers in optimizing RHA content in pervious concrete to enhance both sustainability and performance. This study established the effectiveness of ML models. One of the key limitations of this study was availability of data. While the dataset of 193 observations provides a solid foundation for analysis, it is relatively limited given the inherent variability in concrete properties. Future studies should aim to expand the dataset by including diverse concrete mix designs, variations in RHA particle size, and additional environmental factors to enhance model accuracy and generalizability. This additional information could potentially improve predictive capabilities of ML models. Future research could explore incorporating additional data sources or parameters into ML models. This could involve data on specific properties of RHA used or local environmental conditions to refine prediction accuracy for compressive strength further. Additionally, investigating the explainability of the ML model could provide insights into the vital factors affecting the model's predictions.

Abbreviations

Agg/B	Aggregate to binder ratio
ANN	Artificial Neural Network
BPNN	Backpropagation Neural Networks
BT	Boosted Tree Regression
CNN	Convolutional Neural Network
LR	Linear Regression
ML	Machine learning
NLR	Non-linear Regression

RF	Random Forest Regression
RHA	Rice husk ash
RHA/B	Rice husk ash to binder ratio
SCM	Supplementary cementitious materials
SHAP	SHapley Additive exPlanations
SVR	Support Vector Regression
W/B	Water to binder ratio
XGB	Extreme Gradient Boosting

Acknowledgement

The authors wish to extend their heartfelt thanks to the Department of Civil Engineering at University of Jaffna, for their invaluable support.

Funding Statement

The authors received no specific funding for this study.

CRediT authorship contribution statement

Sathiparan: Conceptualization, Investigation, Formal analysis, Writing – original draft. **Pratheeba**: Conceptualization, Investigation, Formal analysis, Writing – review & editing. **Daniel**: Conceptualization, Investigation, Formal analysis, Writing – review & editing.

Conflicts of Interest

The authors affirm that there are no conflicts of interest to disclose in relation to this study.

References

[1] Dash S, Kar B. Environment friendly pervious concrete for sustainable construction. IOP Conference Series: Materials Science and Engineering. 2018; 410(1): 012005. https://doi.org/10.1088/1757-899X/410/1/012005

[2] Neithalath N, Sumanasooriya MS, Deo O. Characterizing pore volume, sizes, and connectivity in pervious concretes for permeability prediction. Materials Characterization. 2010; 61(8): 802-13. https://doi.org/10.1016/j.matchar.2010.05.004

[3] Alimohammadi V, Maghfouri M, Nourmohammadi D, Azarsa P, Gupta R, Saberian M. Stormwater runoff treatment using pervious concrete modified with various nanomaterials: A comprehensive review. Sustainability. 2021; 13(15): 8552. https://doi.org/10.3390/su13158552

[4] Zhang X, Shen Y, Fan Y, Gao X. Experimental study on the triaxial compression mechanical performance of basalt fiber-reinforced recycled aggregate concrete after exposure to high temperature. Case Studies in Construction Materials. 2024; 20: e03026. https://doi.org/10.1016/j.cscm.2024.e03026

[5] Zhang X, Niu J, Xu P, Deng D, Fan Y. Investigation on eccentric compression performance of basalt fiber-reinforced recycled aggregate concrete-filled square steel tubular columns. Developments in the Built Environment. 2024; 18: 100411. https://doi.org/10.1016/j.dibe.2024.100411

[6] Subramaniam DN, Sathiparan N. Comparative study of fly ash and rice husk ash as cement replacement in pervious concrete: mechanical characteristics and sustainability analysis. International Journal of Pavement Engineering. 2022: 1-18. https://doi.org/10.1080/10298436.2022.2075867

[7] Sathiparan N. Utilization prospects of eggshell powder in sustainable construction material – A review. Construction and Building Materials. 2021; 293: 123465. https://doi.org/10.1016/j.conbuildmat.2021.123465

[8] Lou Y, Khan K, Amin MN, Ahmad W, Deifalla AF, Ahmad A. Performance characteristics of cementitious composites modified with silica fume: A systematic review. Case Studies in Construction Materials. 2023; 18: e01753. https://doi.org/10.1016/j.cscm.2022.e01753

[9] Sathiparan N, Dassanayake DHHP, Subramaniam DN. Utilization of supplementary cementitious materials in pervious concrete: a review. International Journal of Environmental Science and Technology. 2024; 21(6): 5883-918. https://doi.org/10.1007/s13762-023-05440-4

[10] Nilimaa J. Smart materials and technologies for sustainable concrete construction. Developments in the Built Environment. 2023; 15: 100177. https://doi.org/10.1016/j.dibe.2023.100177

[11] Ndahirwa D, Zmamou H, Lenormand H, Leblanc N. The role of supplementary cementitious materials in hydration, durability and shrinkage of cement-based materials, their environmental and economic benefits:

A review. Cleaner Materials. 2022; 5: 100123. https://doi.org/10.1016/j.clema.2022.100123
[12] Wijekoon SH, Shajeefpiranath T, Subramaniam DN, Sathiparan N. A mathematical model to predict the porosity and compressive strength of pervious concrete based on the aggregate size, aggregate-to-cement ratio and compaction effort. Asian Journal of Civil Engineering. 2024; 25(1): 67-79. https://doi.org/10.1007/s42107-023-00757-4
[13] Sonebi M, Bassuoni M, Yahia A. Pervious concrete: mix design, properties and applications. RILEM Technical Letters. 2016; 1(0): 109-15. https://doi.org/10.21809/rilemtechlett.2016.24
[14] Yang L, Kou S, Song X, Lu M, Wang Q. Analysis of properties of pervious concrete prepared with difference paste-coated recycled aggregate. Construction and Building Materials. 2021; 269: 121244. https://doi.org/10.1016/j.conbuildmat.2020.121244
[15] Ziolkowski P, Niedostatkiewicz M. Machine learning techniques in concrete mix design. Materials. 2019; 12(8): 1256. https://doi.org/10.3390/ma12081256
[16] Sathiparan N, Jeyananthan P, Subramaniam DN. Influence of metakaolin on pervious concrete strength: a machine learning approach with shapley additive explanations. Multiscale and Multidisciplinary Modeling, Experiments and Design. 2024; 7(4): 3919-46. https://doi.org/10.1007/s41939-024-00455-x
[17] Sathiparan N, Jeyananthan P, Subramaniam DN. Prediction of compressive strength of fly ash blended pervious concrete: a machine learning approach. Journal of Pavement Engineering. 2023. https://doi.org/10.1080/10298436.2023.2287146
[18] Yu G, Zhu S, Xiang Z. The prediction of pervious concrete compressive strength based on a convolutional neural network. Buildings. 2024; 14(4): 907. https://doi.org/10.3390/buildings14040907
[19] Sudhir Kumar B, Srikanth K, Eeshwar T. Implementation of soft computing techniques in forecasting compressive strength and permeability of pervious concrete blended with ground granulated blast-furnace slag. Journal of Soft Computing in Civil Engineering. 2024; 8(2): 19-45. https://doi.org/10.22115/scce.2023.359399.1517
[20] Sathiparan N, Jeyananthan P, Subramaniam DN. Silica fume as a supplementary cementitious material in pervious concrete: prediction of compressive strength through a machine learning approach. Asian Journal of Civil Engineering. 2024. https://doi.org/10.1007/s42107-023-00956-z
[21] Le B-A, Vu V-H, Seo S-Y, Tran B-V, Nguyen-Sy T, Le M-C, Vu T-S. Predicting the compressive strength and the effective porosity of pervious concrete using machine learning methods. KSCE Journal of Civil Engineering. 2022; 26(11): 4664-79. https://doi.org/10.1007/s12205-022-1918-z
[22] Ahmad SA, Rafiq SK, Hilmi HDM, Ahmed HU. Mathematical modeling techniques to predict the compressive strength of pervious concrete modified with waste glass powders. Asian Journal of Civil Engineering. 2023. https://doi.org/10.1007/s42107-023-00811-1
[23] Feng D-C, Liu Z-T, Wang X-D, Chen Y, Chang J-Q, Wei D-F, Jiang Z-M. Machine learning-based compressive strength prediction for concrete: An adaptive boosting approach. Construction and Building Materials. 2020; 230: 117000. https://doi.org/10.1016/j.conbuildmat.2019.117000
[24] Marani A, Nehdi ML. Machine learning prediction of compressive strength for phase change materials integrated cementitious composites. Construction and Building Materials. 2020; 265: 120286. https://doi.org/10.1016/j.conbuildmat.2020.120286
[25] Sathiparan N, Jeyananthan P. Prediction of masonry prism strength using machine learning technique: Effect of dimension and strength parameters. Materials Today Communications. 2023; 35: 106282. https://doi.org/10.1016/j.mtcomm.2023.106282
[26] Sathiparan N, Jeyananthan P. Predicting compressive strength of cement-stabilized earth blocks using machine learning models incorporating cement content, ultrasonic pulse velocity, and electrical resistivity. Nondestructive Testing and Evaluation. 2023; 39(5): 1054-69. https://doi.org/10.1080/10589759.2023.2240940
[27] Ahsan MB, Hossain Z. Supplemental use of rice husk ash (RHA) as a cementitious material in concrete industry. Construction and Building Materials. 2018; 178: 1-9. https://doi.org/10.1016/j.conbuildmat.2018.05.101
[28] Amin MN, Khan K, Abu Arab AM, Farooq F, Eldin SM, Javed MF. Prediction of sustainable concrete utilizing rice husk ash (RHA) as supplementary cementitious material (SCM): Optimization and hyper-tuning. Journal of Materials Research and Technology. 2023; 25: 1495-536. https://doi.org/10.1016/j.jmrt.2023.06.006
[29] Lo F-C, Lee M-G, Lo S-L. Effect of coal ash and rice husk ash partial replacement in ordinary Portland cement on pervious concrete. Construction and Building Materials. 2021; 286: 122947. https://doi.org/10.1016/j.conbuildmat.2021.122947
[30] Adamu M, Ayeni KO, Haruna SI, Ibrahim Mansour YE-H, Haruna S. Durability performance of pervious concrete containing rice husk ash and calcium carbide: A response surface methodology approach. Case Studies in Construction Materials. 2021; 14: e00547. https://doi.org/10.1016/j.cscm.2021.e00547
[31] Kashem A, Karim R, Das P, Datta SD, Alharthai M. Compressive strength prediction of sustainable concrete

incorporating rice husk ash (RHA) using hybrid machine learning algorithms and parametric analyses. Case Studies in Construction Materials. 2024; 20: e03030. https://doi.org/10.1016/j.cscm.2024.e03030
[32] Adamu M, Olalekan SS, Aliyu MM. Optimizing the mechanical properties of pervious concrete containing calcium carbide and rice husk ash using response surface methodology. Journal of Soft Computing in Civil Engineering. 2020; 4(3): 106-23. https://doi.org/10.22115/scce.2020.229019.1216
[33] Balasubramani V, Jayagamnesh V, Seyamala S. A review on strength properties of pervious concrete using a rice husk ash. SSRG International Journal of Civil Engineering. 2019; SI: 26-29.
[34] Hesami S, Ahmadi S, Nematzadeh M. Effects of rice husk ash and fiber on mechanical properties of pervious concrete pavement. Construction and Building Materials. 2014; 53: 680-91. https://doi.org/10.1016/j.conbuildmat.2013.11.070
[35] Kim Y, Sung C. Void ratio and strength properties of porous concrete utilizing rice husk ash and recycled aggregae for planting. The Journal of Agricultural Science. 2006; 33(2): 167-77.
[36] Jaya RP. Porous concrete pavement containing nanosilica from black rice husk ash. In: Samui P, Kim D, Iyer NR, Chaudhary S (Eds.), New Materials in Civil Engineering, Butterworth-Heinemann, Oxford, 2020; 493-527.
[37] Sai Kumar PP, Jafar SK, Sumanth P, Khan AA, Kumar PS, Kumar TA. Utilization of rice husk ash on pervious concrete as a partial replacement of cement. International Journal of Engineering Sciences & Research Technology. 2020; 9(10): 41-48.
[38] Shafabakhsh G, Ahmadi S. Evaluation of coal waste ash and rice husk ash on properties of pervious concrete pavement. International Journal of Engineering (IJE), TRANSACTIONS B: Applications. 2020; 29(2): 192-201.
[39] Shekhar S, Shukla A. Development of pervious paver block by using rap and rice husk ash. International Journal for Research in Applied Science & Engineering Technology. 2020; 11(10): 1019-33.
[40] Shwetha J. Experimental study on pervious concrete using fly ash and rice husk ash. International Journal of Engineering Research in Mechanical and Civil Engineering. 2022; 9(4): 1-3.
[41] Talsania S, Pitroda J, Vyas C. Effect of rice husk ash on properties of pervious concrete. International Journal of Advanced Engineering Research and Studies. 2015; 4(2): 296-9.
[42] Vanathi D, Radhika DK, Swetha MG. A sustainable study on permeable concrete using bagasse ash and rice husk ash as a partial replacement of cement. E3S Web Conference, Yogyakarta, 2020; 184: 01083.
[43] ASTM-C39/C39M. Standard test method for compressive strength of cylindrical concrete specimens. West Conshohocken, PA: ASTM International, 2021.
[44] BS-EN-12390-3. Testing hardened concrete - Compressive strength of test specimens. London: British Standards Institution (BSI), 2019.
[45] IS-516. Method of tests for strength of concrete. New Delhi: Bureau of Indian Standards (BIS), 1959.
[46] Seifeddine K, Amziane S, Toussaint E. State of the art on the mechanical properties of pervious concrete. European Journal of Environmental and Civil Engineering. 2022; 26(15): 7727-55. https://doi.org/10.1080/19648189.2021.2008511
[47] Ahmad SA, Rafiq SK. Numerical modeling to predict the impact of granular glass replacement on mechanical properties of mortar. Asian Journal of Civil Engineering. 2024; 25(1): 19-37. https://doi.org/10.1007/s42107-023-00753-8
[48] Bui DK, Nguyen T, Chou JS, Nguyen-Xuan H, Ngo TD. A modified firefly algorithm-artificial neural network expert system for predicting compressive and tensile strength of high-performance concrete. Construction and Building Materials. 2018; 180: 320-33. https://doi.org/10.1016/j.conbuildmat.2018.05.201
[49] Subramaniam DN, Jeyananthan P, Sathiparan N. Soft computing techniques to predict the electrical resistivity of pervious concrete. Asian Journal of Civil Engineering. 2023. https://doi.org/10.1007/s42107-023-00806-y
[50] Nohara Y, Matsumoto K, Soejima H, Nakashima N. Explanation of machine learning models using shapley additive explanation and application for real data in hospital. Computer Methods and Programs in Biomedicine. 2022; 214: 106584. https://doi.org/10.1016/j.cmpb.2021.106584
[51] John E, Lothenbach B. Cement hydration mechanisms through time – A review. Journal of Materials Science. 2023; 58(24): 9805-33. https://doi.org/10.1007/s10853-023-08651-9